Electronic Supplementary Material (ESI) for ChemComm.
This journal is © The Royal Society of Chemistry 2016

Electronic supplementary information (ESI) for

Three-Dimensional Accordion-Like Metal–Organic Framework: Synthesis and Unconventional Oriented Growth on Surface

Tomoyuki Haraguchi,[a] Kazuya Otsubo,[*,a] Osami Sakata,[b] Shogo Kawaguchi,[c] Akihiko Fujiwara,[d] and Hiroshi Kitagawa,[*,a,e,f]

[a]Division of Chemistry, Graduate School of Science, Kyoto University, Kitashirakawa-Oiwakecho, Sakyo-ku, Kyoto 606-8502, Japan

[b]Synchrotron X-ray Station at SPring-8, National Institute for Materials Science (NIMS), 1-1-1 Kouto, Sayo-cho, Sayo-gun, Hyogo 679-5148, Japan

[c]Japan Synchrotron Radiation Research Insitute (JASRI), SPring-8 1-1-1 Kouto, Sayo-cho, Sayo-gun, Hyogo 679-5198, Japan.

[d]School of Science and technology, Kwansei Gakuin University, 2-1 Gakuen, Sanda, Hyogo 669-1337, Japan

[e]Institute for Integrated Cell-Material Sciences (iCeMS), Kyoto University, Yoshida, Sakyo-ku, Kyoto 606-8501, Japan

[f]INAMORI Frontier Research Center, Kyushu University, 744 Motooka, Nishi-ku, Fukuoka 819-3095, Japan

*email: kazuya@kuchem.kyoto-u.ac.jp; kitagawa@kuchem.kyoto-u.ac.jp

Table of Contents

1. Experimental details

Materials: 4-mercaptopyridine, $Fe(BF_4)_2 \cdot 6H_2O$, $(NH_4)_2Fe(SO_4)_2 \cdot 6H_2O$, $K_2[Pt(CN)_4] \cdot H_2O$, $[(C_4H_9)_4N]ClO_4$, 4,4′-bypridine (bpy), ethanol (EtOH), and methanol (MeOH) were purchased from Tokyo Kasei Kogyo Co. Ltd., Sigma-Aldrich Chemical Co., or Kishida Chemical Co. Ltd. These materials were used without any purification. The substrate (Au/Cr/Si) was purchased from Nilaco Corp. It was prepared by evaporating 5 nm of chromium, followed by 100 nm of gold, onto polished silicon wafers. The substrate was used after washing with pure EtOH and H_2-annealing treatment. The starting substance $[(C_4H_9)_4N]_2[Pt(CN)_4]$ was prepared by the cation-exchange reaction of $K_2[Pt(CN)_4]$ and $[(C_4H_9)_4N]ClO_4$ in EtOH for a few days.

Synthesis of 1: A water/MeOH (1:1) solution containing $K_2[Pt(CN)_4] \cdot H_2O$ (202.9 mg, 9 mM) and bpy (84.7 mg, 9 mM), and a water solution containing $(NH_4)_2Fe(SO_4)_2 \cdot 6H_2O$ (182.9 mg, 9 mM) were diffused in an H-shaped glass tube. After several weeks, yellow plate-like single crystals were obtained. Elemental analysis (%). Calc. for $C_{14}H_8N_6FePt \cdot 3H_2O$: C, 29.75; H, 2.50; N, 14.87. Found: C, 29.44; H, 2.35; N, 14.79.

Crystallographic data for 1: Mr = 543.20, crystal size = 0.30 × 0.30 × 0.10 mm^3, monoclinic, space group C2/*c* (no. 15), a = 15.667(2) Å, b = 15.136(2) Å, c = 7.3104(11) Å, β = 110.570(2)°, V = 1623.0(4) $Å^3$, Z = 4, d_{calc} = 2.223 g/cm^3, F(000) = 1016, μ = 9.523 mm^{-1}, T = 300(2) K. A total of 1817 reflections were collected, 1626 of which were unique (R_{int} = 0.1483). Refinement of 112 parameters led to the final R_1 = 0.0501 ($I > 2\sigma(I)$), wR_2 = 0.1257 (all data), goodness of fit = 1.088, and residual electron density max/min = 4.100/–2.807 e $Å^{-3}$. CCDC reference number: 1444414.

Fabrication of film-1: First, the substrate was immersed in an EtOH solution of 4-mercaptopyridine (1 mM) overnight. Thereafter, the substrate was washed with pure EtOH and dried under nitrogen gas flow. Formation of the self-assembled monolayers (SAMs) was monitored by quartz crystal microbalance (QCM) measurements. Then, the substrate was alternately immmersed in EtOH solutions of $Fe(BF_4)_2 \cdot 6H_2O$ (100 mM), $[(C_4H_9)_4N]_2[Pt(CN)_4]$ (100 mM), bpy (100 mM) for 1 min. at −60℃ for 30 steps. The

substrate was washed with pure EtOH after every immersing.

Method: Single-crystal X-ray diffraction data of **1** was collected on a Bruker SMART APEX CCD (charge-coupled device) area detector with graphite-monochromated Mo Kα radiation. The thermogravimetric analysis of **1** was performed using a NETZSCH Japan TG-DTA 2,000SA with a heating rate of 2 K per min under N_2 gas flow. The magnetic susceptibility of **1** was measured using Quantum Design SQUID magnetometers (MPMS-XL5) in the Research Center for Low Temperature and Materials Sciences, Kyoto University, Japan. The contributions of the sample holder were subtracted by blank experiments. The core diamagnetic susceptibility of **1** was estimated using Pascal's table to be -2.49×10^{-4} emu/mol. Infrared reflection absorption spectra (IRRAS) data were collected using a NEXUS 670 FT-IR apparatus (Thermo Nicolet). Raman spectra measurements were carried out using a NRS-1000 apparatus (Jasco) with He-Ne laser (λ = 632 nm). Synchrotron X-ray diffraction (XRD) measurements were carried out for **film-1** using a multi-axis diffractometer (Kohzu-Seiki TDT-17) with a scintillation detector installed on the BL13XU beamline of SPring-8. The incident X-ray was monochromatized to 8 keV (λ = 1.550 Å) with a Si111 double-crystal monochromator. Helium gas was supplied during the measurements. Out-of-plane XRD measurement was performed in a typical θ–2θ scattering geometry. Azimuth angle dependence measurements were performed at 110 peak position in the out-of-plane geometry. In grazing-incidence XRD (GIXRD, in-plane mode), strong scattered intensity can be observed when the X-ray incident angle (α) to the sample is below a critical angle. Thus, the GIXRD measurement at the 111 peak position was performed before the in-plane XRD measurement, and the diffraction patterns were collected at α = 0.2°. A Soller slit (Huber 3030-I, 0.4°) was placed between the sample substrate and the scintillation detector to reduce scatter background from the diffraction. XRD pattern fittings shown in Fig. 2 were performed using Topas program.[S1] Simulated XRD patterns shown in Fig. 2 were obtained with the Mercury software suite.[S2] In the case of in situ XRD measurements of **film-1**, the vapour pressure was constantly introduced into the sample cell using a BEL-Flow system. Atomic force microscopy (AFM) images of **film-1** were obtained by tapping mode equipped with NanoScope IIIa system (Veeco Instrument Inc.). The sorption properties of **film-1** were investigated by quartz crystal microbalance (QCM) measurements with a BELQCM system (MicrotracBEL). Before the measurements, the QCM sensors were activated at 80 °C for 1h under helium gas flow inside the QCM chamber. Adsorption and desorption isotherm measurements of **1** were performed with a

BELSORP-max apparatus (MicrotracBEL). **1** was degassed at 413 K for a day as preliminary preparation. Synchrotron Powder X-ray diffraction measurements of **1** were carried out on the BL02B2 beamline of SPring-8 (λ = 0.688 Å). The XRD patterns of **1** sealed in glass capillaries under MeOH and H_2O saturated vapours were measured at RT. All of the XRD patterns were obtained with a 0.01° step. The cell parameters were determined by Le Bail analysis with Topas program.[S1] The lattice parameters of **1** obtained by single crystal analysis (monoclinic, *C*2/*c*, *a* = 15.667(2) Å, *b* = 15.136(2) Å, *c* = 7.310(1) Å and β = 110.570(2)°) were used as starting parameters for the fitting.

2. Thermogravimetric analysis of bulk sample

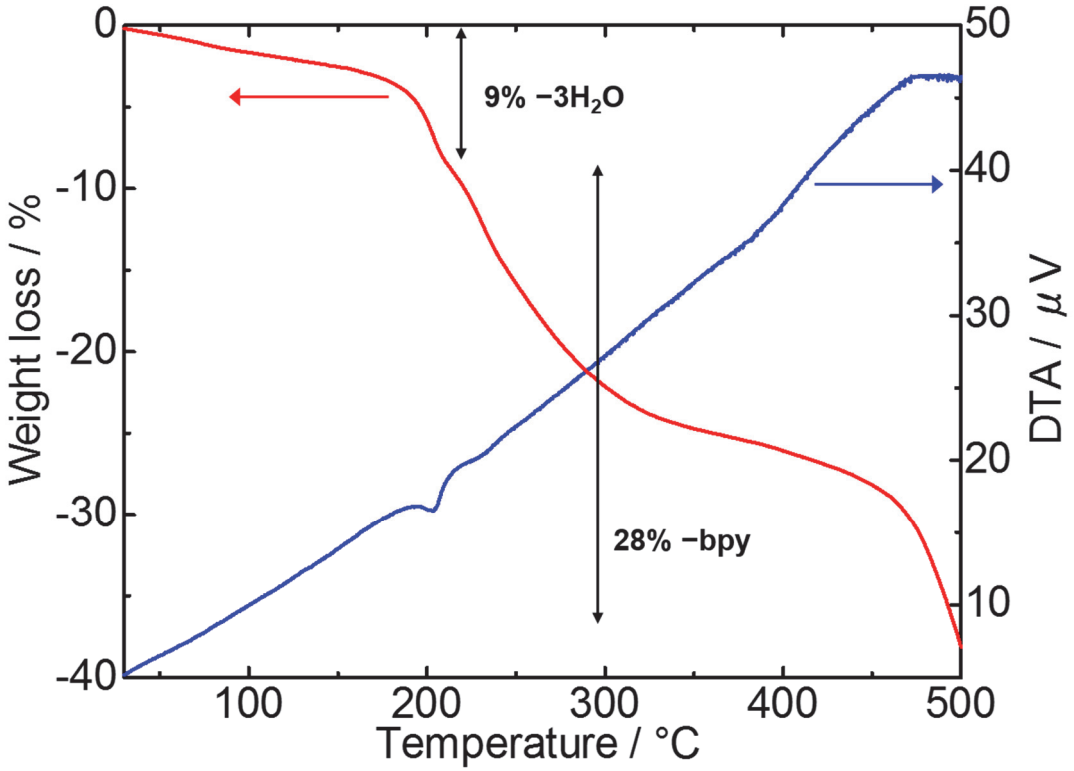

Fig. S1 Thermogravimetric analysis curve of **1** under N_2 flow. Desorption of two coordination water after desorption of one crystal water was observed.

3. Fitting of $\chi_M T$–T curve for bulk sample

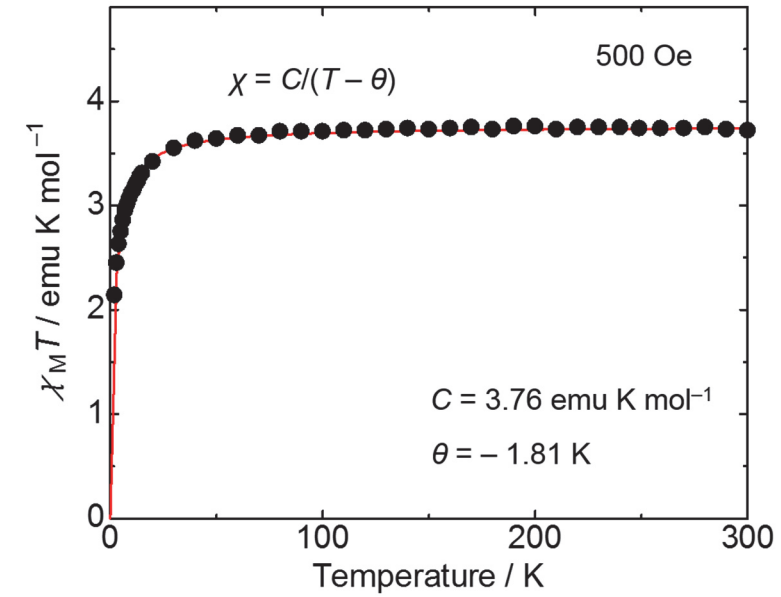

Fig. S2 Temperature T dependence of the molar magnetic susceptibility χ_M ($\chi_M T$–T curve) of **1** measured in an external field of 500 Oe. Filled circles and the red line denote experimental data and fitting results, respectively.

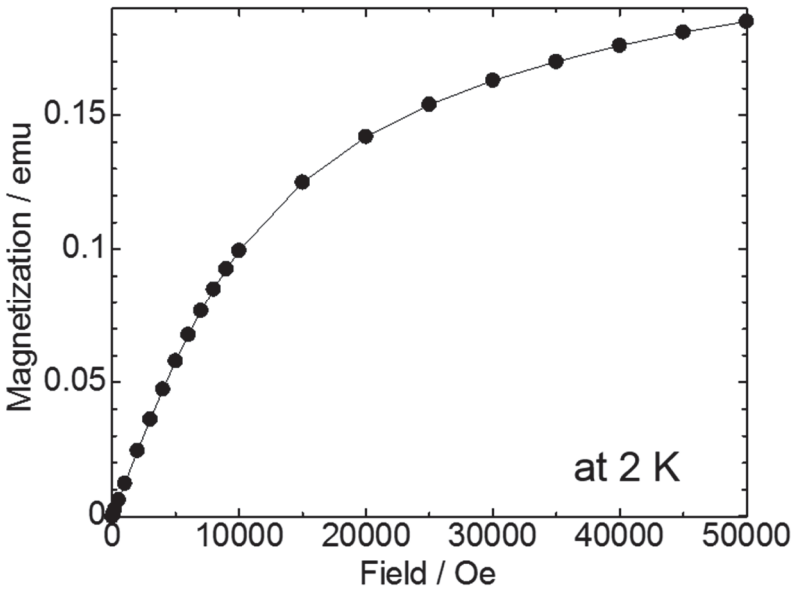

Fig. S3 Magnetization–external magnetic field curve at 2 K.

4. Sorption properties of bulk sample

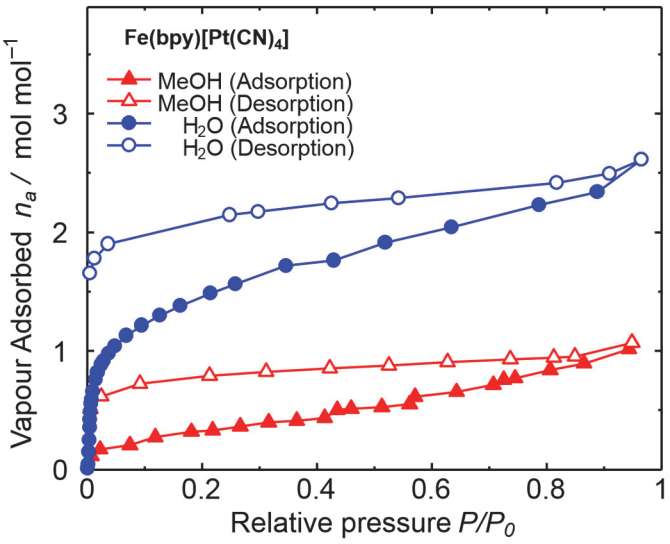

Fig. S4 Sorption isotherms of **1** at RT. Filled symbols and open symbols denote adsorption and desorption, respectively.

5. IRRAS and Raman spectra

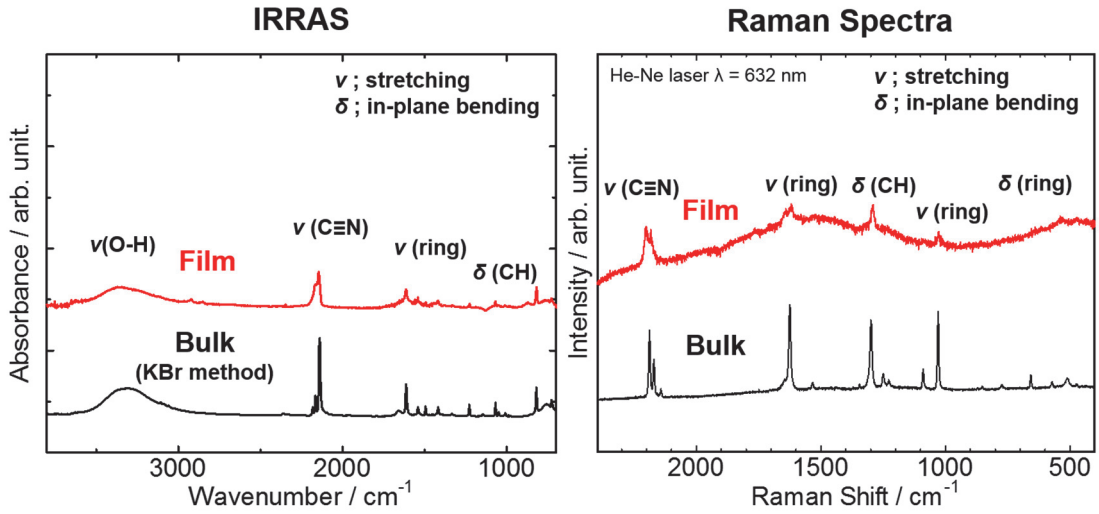

Fig. S5 Infrared reflection absorption spectra (IRRAS) and Raman spectra of **film-1** and **1**. **film-1** (redline) and **1** (black line) showed the same IRRAS and Raman spectra.

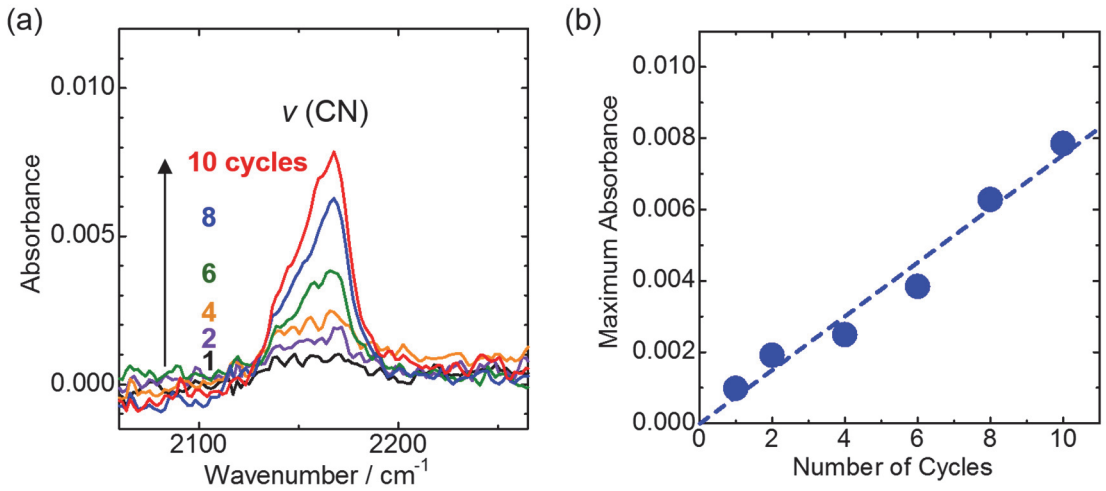

Fig. S6 Thin film growth monitoring by IRRAS measurements. Maximum absorbance of CN stretching mode ν(CN) showed a linear increase according to the number of cycles, which implies that the thin film thickness can be controlled by the number of cycles.

6. Schematic representation of (110) diffraction planes

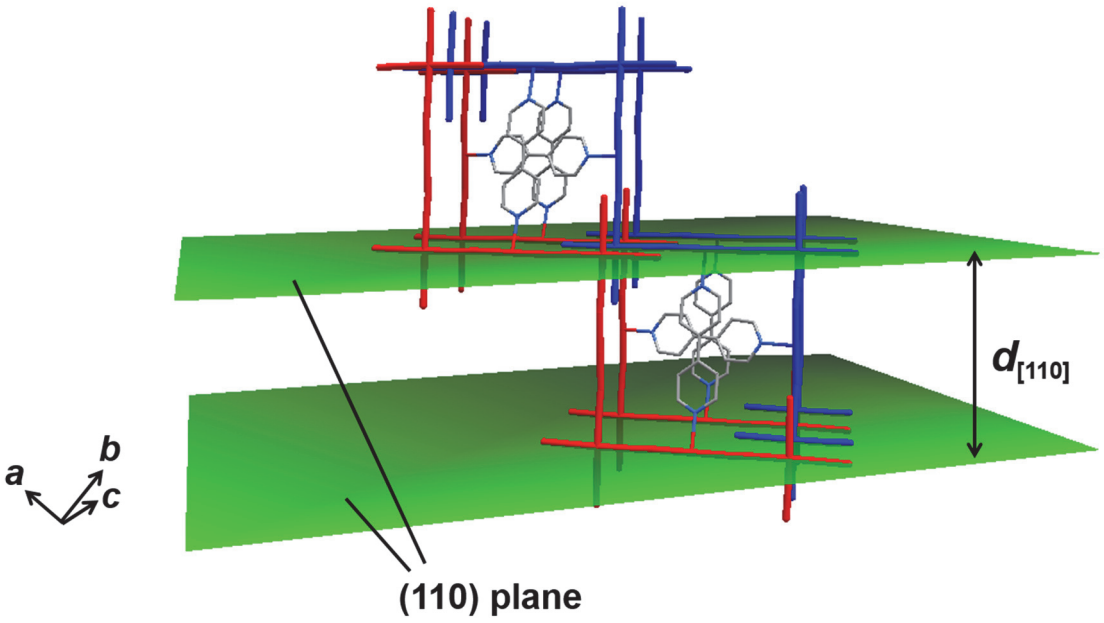

Fig. S7 Schematic representation of (110) diffraction planes for **1**. The *d*-spacing calculated from (110) diffraction planes, $d_{[110]}$, is also indicated.

7. Rocking curve and azimuth angle scans

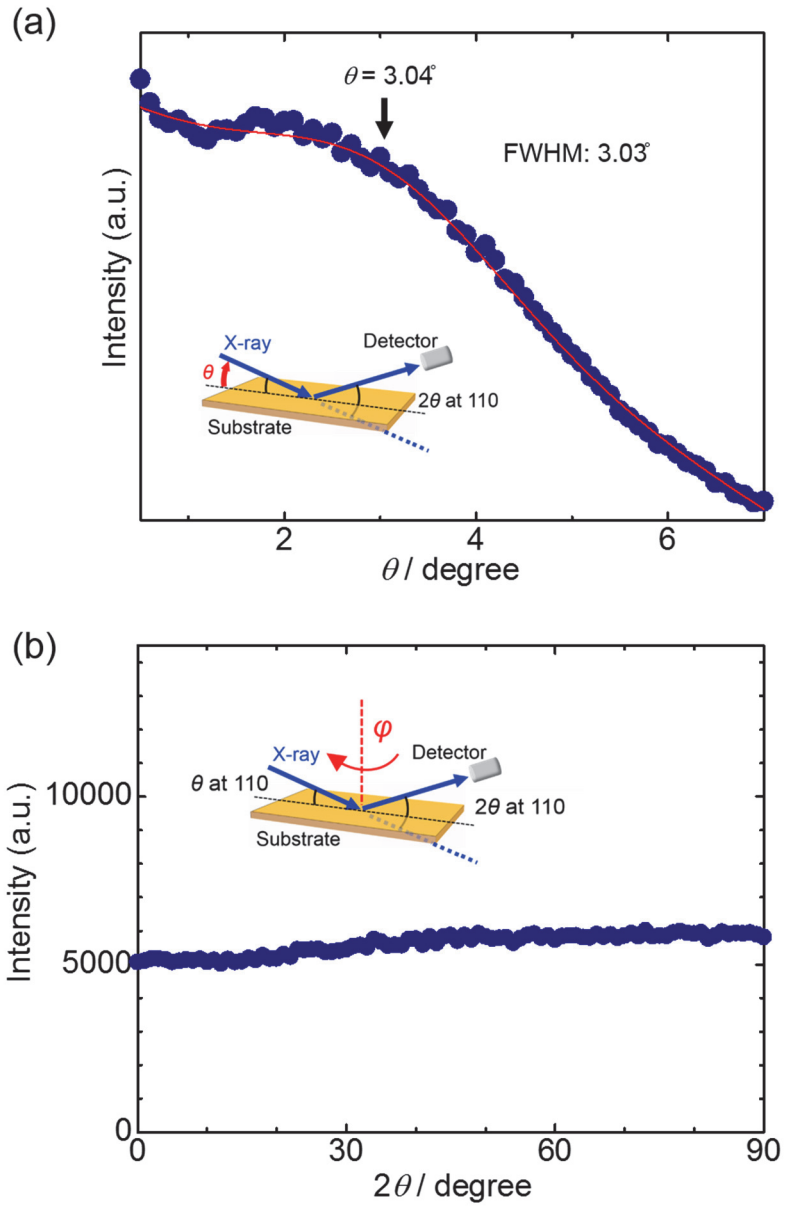

Fig. S8 Rocking curve scan (a) and azimuthal-angle scan (b) at 110 position for **film-1**. The absence of peak intensity dependence on the azimuth angle implies that the thin film is uniformly fabricated on the substrate.

8. AFM image of the thin film

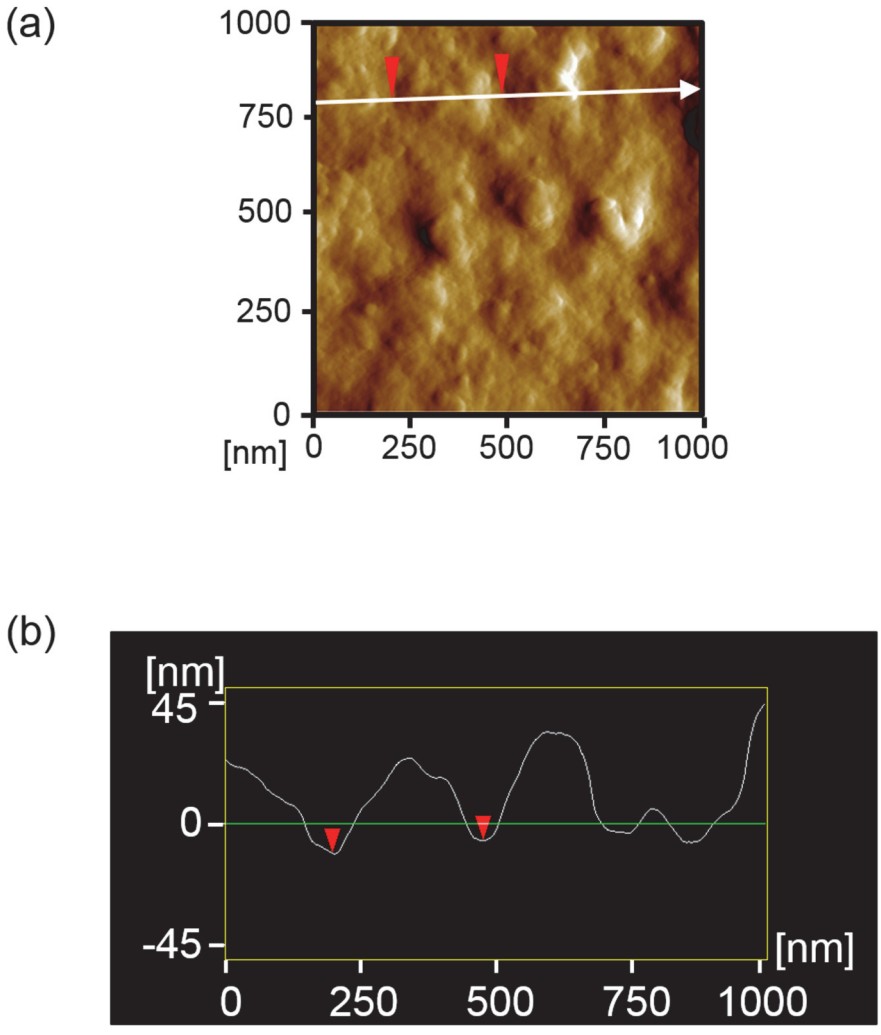

Fig. S9 AFM image of the **film-1** at RT. (a) amplitude mode and (b) section analysis.

9. *In situ* in-plane XRD experiments

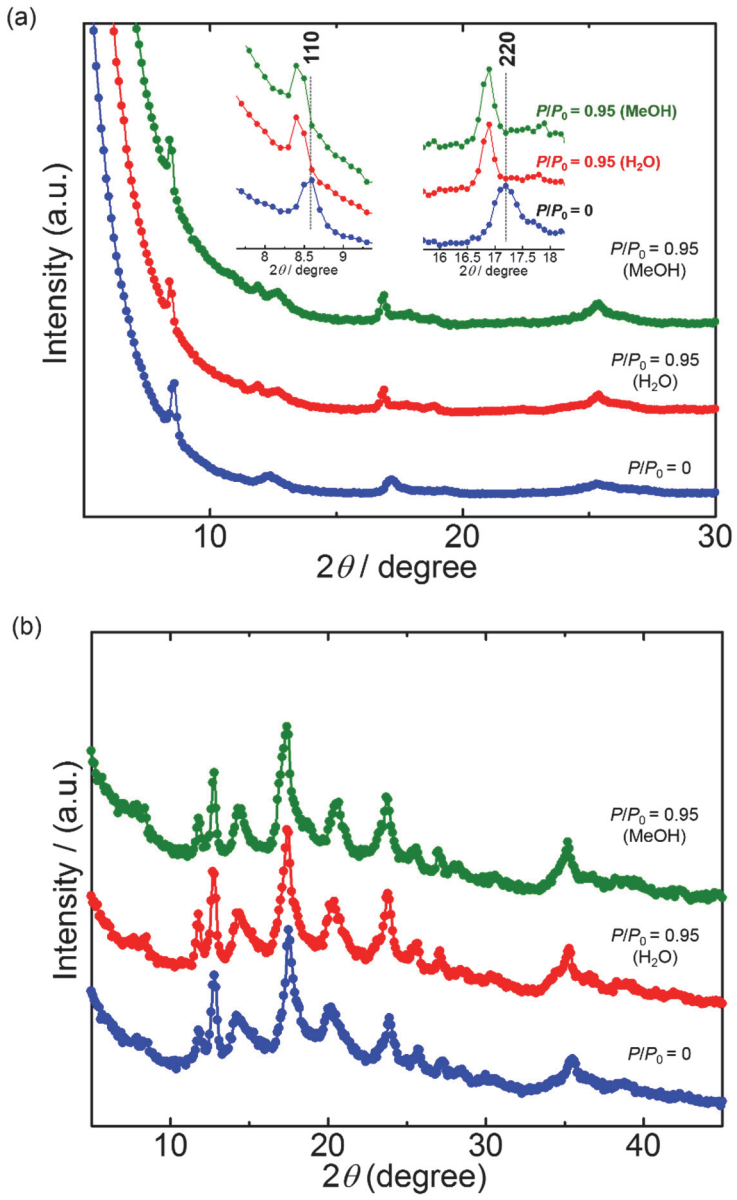

Fig. S10 *In situ* XRD measurement of **film-1** under MeOH and H_2O vapours at RT: (a) out-of-plane and (b) in-plane. There is almost no peak shift seen in the in-plane patterns.

10. Synchrotron powder XRD measurements of bulk sample

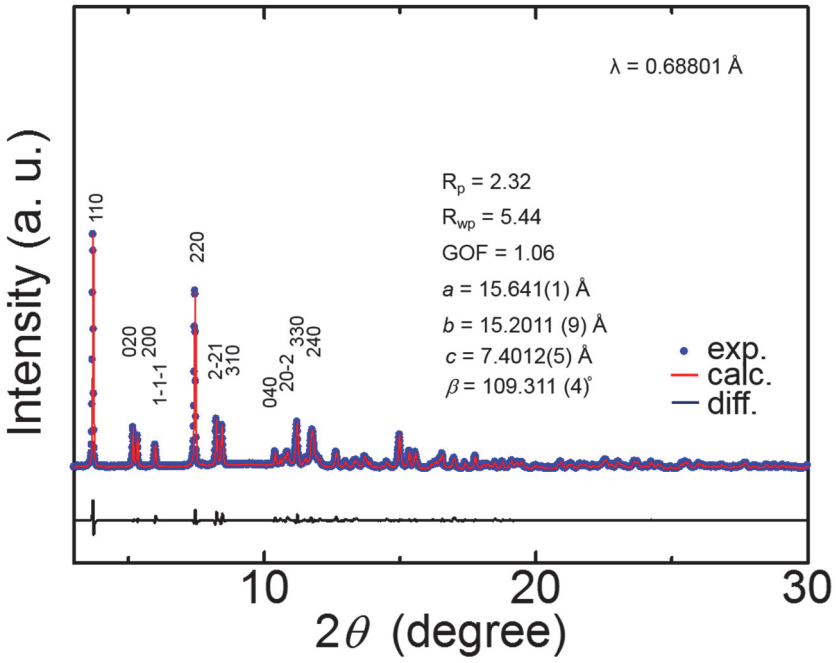

Fig. S11 Le Bail analysis in C2/*c* of the pattern of **1** (as-synthesized) at RT.

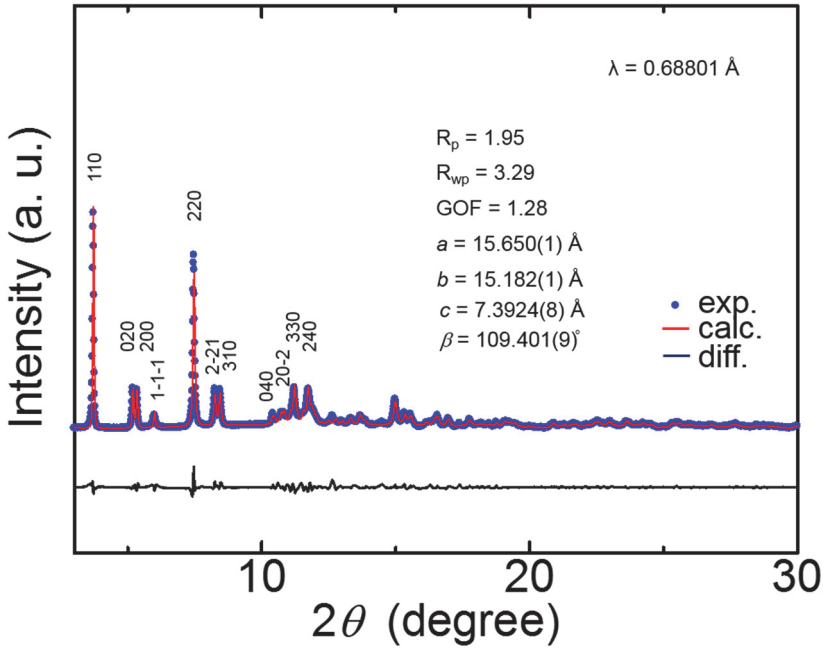

Fig. S12 Le Bail analysis in C2/*c* of the pattern of **1** (activated) at RT.

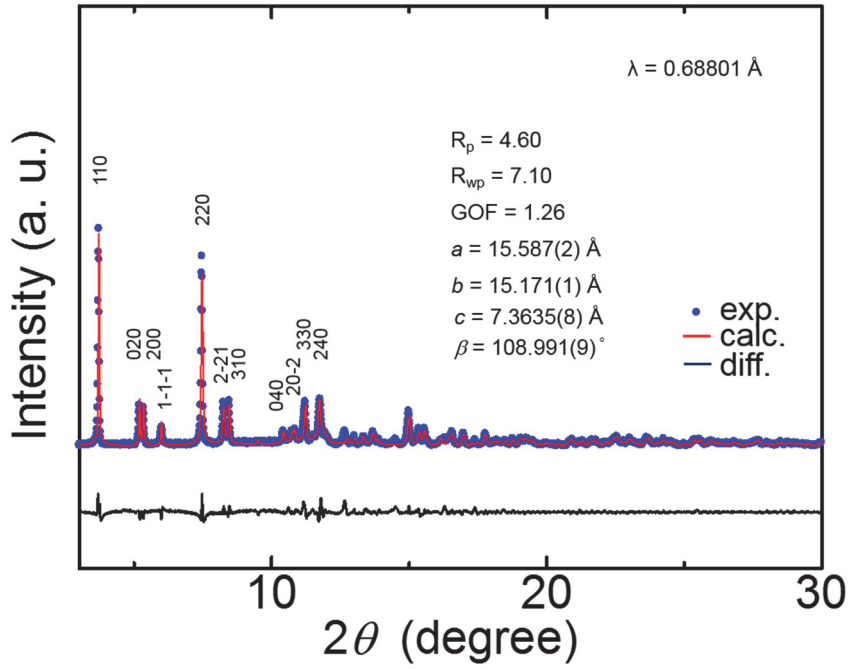

Fig. S13 Le Bail analysis in C2/*c* of the pattern of **1** (under MeOH saturated vapour) at RT.

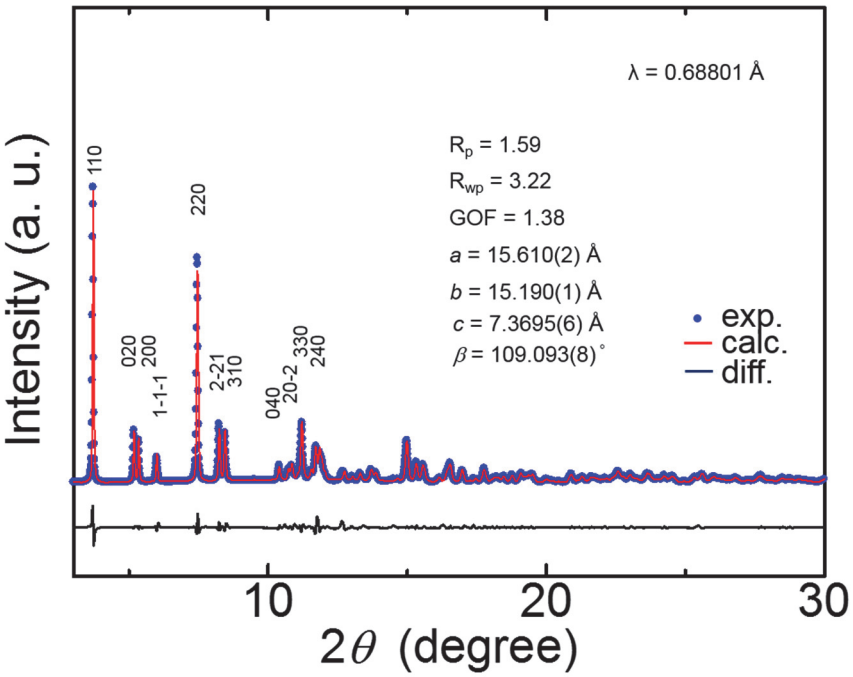

Fig. S14 Le Bail analysis in C2/*c* of the pattern of **1** (under H_2O saturated vapour) at RT.

Table S1. Cell parameters of **1** under various saturated vapours.

	a / Å	*b* / Å	*c* / Å	β / degree	d_{110} / Å	*V* / Å^3
As-synthesized	15.641(1)	15.2011(9)	7.4012(5)	109.311(4)	10.5898(4)	1661.8(2)
Activated	15.650(1)	15.182(1)	7.3924(8)	109.401(9)	10.5834(5)	1656.7(3)
MeOH	15.587(2)	15.171(1)	7.3635(8)	108.991(9)	10.5713(8)	1646.5(3)
H_2O	15.610(2)	15.190(1)	7.3695(6)	109.093(8)	10.5824(7)	1651.3(3)

11. Cell parameters of bulk sample and thin film

Table S2. Comparison of cell parameters of **film-1** and **1** (activated).

	a / Å	*b* / Å	*c* / Å	β / degree	d_{110} / Å	*V* / Å^3
Bulk	15.650(1)	15.182(1)	7.3924(8)	109.401(9)	10.5834(5)	1656.7(3)
Film	15.59(1)	15.185(9)	7.095(6)	108.2(1)	10.43(4)	1596(2)
$(x_{Bulk}-x_{Film})/x_{Bulk}$	0.0038(6)	-0.0002(6)	0.0402(8)	0.0109(9)	0.015(4)	0.037(1)

12. References

S1. Bruker AXS, *TOPAS V3*: General profile and structure analysis software for powder diffraction data, Bruker AXS, Karlsruhe, Germany, **2005**.

S2. Mercury: visualization and analysis of crystal structures, Macrae, C. F.; Edgington, P. R.; McCabe, P.; Pidcock, E.; Shields, G. P.; Taylor, R.; Towler, M.; van de Streek, J. *J. Appl. Cryst.* **2006**, 39, 453.